The International Journal of Advanced Manufacturing Technology (2022) 121:3903–3917
https://doi.org/10.1007/s00170-022-09576-4

ORIGINAL ARTICLE

Robust RFID tag design for reliable communication within the Internet of Things

James Tribe[1] · Steven Hayward[1] · Katherine van Lopik[1] · William G. Whittow[1] · Andrew A. West[1]

Received: 25 February 2022 / Accepted: 17 June 2022 / Published online: 28 June 2022

Abstract

Radio frequency identification (RFID) is a cost-effective method to support the Industrial Internet of Things (IIoT) and is an enabling technology for Industry 5.0. The use of RFID is particularly suited to IIoT as it does not require a line of sight for communication and can be retroactively affixed to non-smart items. However, RFID communication is affected by the properties of the material the tag is affixed to, specifically the material permittivity. Metal is commonly present in smart factory environments and supply chains and impedes RFID communication. A suitable tag design is required to accommodate these challenges and ensure resilience for Industry 5.0 applications. The research presented in this paper has assessed the communication performance of RFID antenna designs with and without metal present beneath the tag. The RFID tag designs that performed reliably in the simulation were manufactured, and their read range was tested on materials of varying relative permittivity and thickness to represent MP and NMP scenarios. The results have verified the robustness of "Cyber" to "Physical" designs and provide recommendations to support practitioner IIoT tag selection.

Keywords Dielectrics · Internet of Things · Radio frequency Identification · Performance verification · Simulation · Digital twin

1 Introduction

The fifth industrial revolution, Industry 5.0, focuses on human-centred, resilient and sustainable smart manufacturing systems [1] and is enabled by the collaboration between cyber and physical systems to optimise production and reduce waste forming a Cyber Physical System (CPS) [2]. Industry 5.0 requires accurate tracking and monitoring of physical assets with communication via the Industrial Internet of Things (IIoT) [1]. Due to the low cost and ease of implementation, radio frequency identification (RFID) has been identified as an enabling technology for Industry 5.0 [1]. RFID tags have been utilised in numerous applications including supply-chain management [3], logistics [4] and location positioning [5, 6]. Although *active* and *semi-active* RFID tags provide greater range and location accuracy [7, 8], they are more expensive and require an on-board power source. The significant cost savings of passive RFID has resulted in wider adoption in industry and selection for reliable IIoT communication [7, 9].

Many factors impact RFID performance including (i) the antenna and microchip, (ii) the casing, (iii) the application environment and (iv) the RFID reader and antenna design; this paper focuses on the tag casing and antenna design to mitigate the impact of metallic objects in the application environment. Metals affect frequency response, input impedance and gain by causing changes to the reactance of the RFID tag [10]. Metal products, components and machines in industrial environments pose a challenge for developing reliable communication using RFID. The RFID tag design must compensate for the effects of the materials the tag is deployed to track; this can be achieved using a dielectric

✉ Steven Hayward
s.hayward@lboro.ac.uk

James Tribe
James.tribe@sky.com

Katherine van Lopik
k.van-lopik@lboro.ac.uk

William G. Whittow
W.G.Whittow@lboro.ac.uk

Andrew A. West
a.a.west@lboro.ac.uk

[1] The Wolfson School of Mechanical Electrical and Manufacturing Engineering, Loughborough University, Loughborough, Leicestershire, UK

spacer. Dielectric spacers offer a robust and cost-effective solution for IIoT applications adopting RFID within harsh, cost-sensitive manufacturing supply chains [11].

For manufacturing applications, understanding the range of effective distances that an antenna can be located relative to tagged products is essential to determine the practicalities and cost-effectiveness of deployments [12]. Hence determining how, and to what extent, the properties of materials affect the performance of antennas is essential to quantifying the cost-effectiveness of RFID solutions within manufacturing supply chains and to ensure technology resilience against disruption for industry 5.0 [1]. Two key application areas where this is imperative are production planning and product tracking and recall, particularly for metallic goods such as engines within automotive manufacturing, as highlighted in [13]. Practically, however, physical testing of all variants of tag design and substrate combination can be prohibitively costly (in terms of time and production of tags).

The ability to design and evaluate an RFID tag in cyber or simulation space enables low-cost, reliable deployment in the physical space. Simulation may be used to demonstrate return on investment or narrow the suitable tag selection pool. However, because simulations use simplified models of reality, they must be accompanied by real-world (physical) testing to ensure robustness. The research reported in this paper has evaluated the efficacy of dielectric materials to enhance the performance of RFID tags in simulation and physical testing.

The paper is structured as follows: To provide a context of the results, a summary of related theory is presented in Sect 1.1. Section 2 outlines the methods used for evaluating the RFID tag performance through simulation and physical testing. The results are presented and discussed in Sect. 3. The conclusions, limitations, future work and practical implications of the research are presented in Sect. 4.

1.1 Related theory

The factors affecting the efficacy of RFID tags are (i) the substrate they are in direct contact with, (ii) the thickness of that substrate and (iii) the distance above a ground plane if present. When an RFID tag is placed onto a substrate, the dielectric properties affect the frequency response and impedance matching properties of the antenna. The placement and position of the tag on the product is important and should be managed through implementing a controlled attachment process. The substrate is attached to one side of the antenna whilst air surrounds the other. The effective dielectric constant of the tag is represented by an average of the dielectric constant of the substrate, ε_r, and that of the air around it (1.00059 ≈ 1) [14]. Therefore, the effective permittivity (ε_{eff}), when there is no ground plane, can be calculated using the following equation [15]:

$$\varepsilon_{eff} = \frac{\varepsilon_r + 1}{2} \tag{1}$$

When an antenna is placed on a dielectric substrate above a ground plane (e.g. a metal product), the radio frequency (RF) fields will be stronger within the dielectric [16] rendering Eq. (1) unsuitable for calculating ε_{eff}. The implication of ground planes enhancing RF performance means viable manufacturing solutions require the investigation of antennas that employ a dielectric and ground plane [17].

Dielectrics are typically used in a microstrip antenna [16] in the form of a *patch* above a *ground plane* separated by a *dielectric*; see Fig. 1. The ground plane introduces *fringing effects* that make the antenna appear *electrically longer* than it is physically [18]. These effects can be accommodated by using an ε_{eff} calculated using Eqs. (2) or (3) depending on the ratio of the width of the patch to the height of the dielectric [18].

In Eqs. (2) and (3), ε_r is the relative permittivity of the substrate, W is the track width and H is the substrate thickness. Changing the ε_r of the material an antenna is attached to will change the resonant frequency of that antenna and hence affect the impedance matching at the operational frequency, resulting in increased signal losses and read range reduction for the tag.

$$\text{For } \frac{W}{H} < 1 \qquad \varepsilon_{eff} = \frac{\varepsilon_r + 1}{2} + \frac{\varepsilon_r - 1}{2} \left[\frac{1}{\sqrt{1 + \frac{12H}{W}}} + 0.04\left(1 - \frac{W}{H}\right)^2 \right] \tag{2}$$

$$\text{Else} \qquad \varepsilon_{eff} = \frac{\varepsilon_r + 1}{2} + \frac{\varepsilon_r - 1}{2} \left[\frac{1}{\sqrt{1 + \frac{12H}{W}}} \right] \tag{3}$$

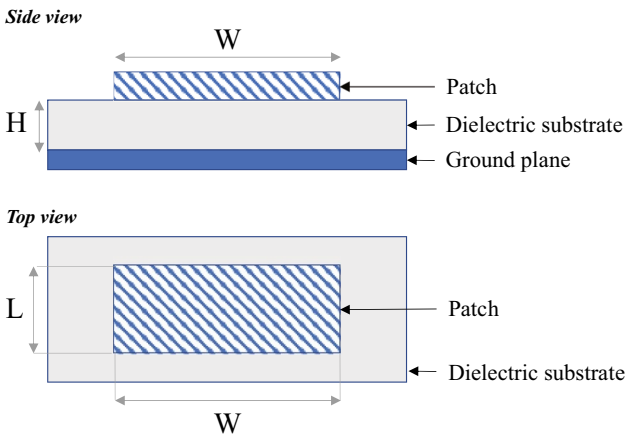

Fig. 1 Microstrip antenna model

2 Method for cyber design and physical testing

Simulations were created and carried out using the EMPIRE XPU electromagnetic software package [19] for tags placed with metal present (NMP) and no metal present (NMP). The simulation results were used to inform the selection of tags for physical testing. Physical testing was conducted in a laboratory environment.

2.1 Simulation/cyber testing

Two scenarios were evaluated with varying dielectric substrates: (i) MP and (ii) NMP. All other variables were kept constant.

For the MP test, the RFID tag antenna is located above a rectangular metal component $160 \times 30 \times 1$ mm^3 with a dielectric material 160×30 mm^2 of variable thickness (0.5 mm, 1 mm, 2 mm, 4 mm, 6 mm, 8 mm and 10 mm). The ε_r of the dielectric was varied from 1 to 5 in steps of 1 to represent a variety of typical dielectric materials used in antenna manufacture (e.g. FR4 and RT Duroid). The antenna was coupled to a source with a resistance of 30.38 Ω in series with a 0.85 pF capacitor to represent the complex impedance 30.53—j211.81 Ω of the Alien Higgs 3 RFID chip [20] at a frequency of 868 MHz, the regulated ultra-high frequency (UHF) RFID frequency in Europe.

The antenna designs evaluated were (i) commercially available Alien Technology squiggle RFID tag (one standard variant) [21], (ii) nested slot antenna (six variations) and (iii) T-match dipole antenna (two variations) [22]. The Alien technology squiggle tag was chosen commercial option due to its widespread adoption, ease of use and its specified read range of up to 12 m [21]. The nested slot antenna has demonstrated robust operation on different materials (e.g. see [23]) and is easily tuneable to different ε_r values. The T-match dipole was chosen as a common antenna for RFID tags which is easy to design and impedance matches the RFID chip.

2.1.1 Matching RFID tag antennas on different materials

To limit the number of simulated ε_r values, antenna matching was carried out using substrates with ε_r values of 1, 3 and 5 to give options across the permittivity values of typical dielectrics (e.g. air/polyurethane foam (1), silicone/polystyrene (3) and glass (5)) used in the simulations. Discrete thicknesses were used to give a range of achievable substrates (i.e. 2 mm, 6 mm and 10 mm, respectively) without the structure becoming too obtrusive for attaching to a product. Loss tangents typically range from a worst case of 0.001 for low loss to 0.01 for lossy materials (e.g. plastic) [24]. The substrate loss tangent for all the antenna simulations was set to the worst case for a dielectric at 0.01.

Table 1 Six nested slot tag antennas designed to achieve S11 < − 15 dB

Antenna name	Substrate description			Optimised dimensions	
	ε_r	Thickness t (mm)	Ground plane?	L (mm)	l(mm)
Slot: $\varepsilon_r = 1$, $t = 2$ mm	1	2	No	147	39
Slot: $\varepsilon_r = 1$, $t = 2$ mm ***M***	1	2	Yes	163	19.5
Slot: $\varepsilon_r = 3$, $t = 6$ mm	3	6	No	125	36
Slot: $\varepsilon_r = 3$, $t = 6$ mm ***M***	3	6	Yes	97	20.5
Slot: $\varepsilon_r = 5$, $t = 10$ mm	5	10	No	100	32
Slot: $\varepsilon_r = 5$, $t = 10$ mm ***M***	5	10	Yes	74	24

A total of six slot tag antenna designs were used (see Table 1). The antenna names have three possible terms at the end to represent the design parameters. The first parameter (ε_r) is the relative permittivity of the substrate material the tag was designed for. The second parameter (t) is the thickness of the antenna substrate. Note that for antennas in the MP scenario below the substrate, this is also the distance between the antenna and the metal. The final optional parameter (***M***) indicates tags designed for metal.

The S11 parameter represents the reflection coefficient and is one of the standard indicators of antenna performance to identify when a good impedance match between the RFID chip and antenna is achieved. For each substrate parameter on the slot tag (Fig. 2), the lengths of the antenna L and slot l were adjusted in repeated simulations until an S11 less than − 15 dB was achieved. To reduce the computational complexity, the slot width (w *in* Fig. 2) and antenna width (W in Fig. 2) were kept constant at 2 mm and 20 mm, respectively (as used in [23]).

The two T-match dipole designs (Fig. 3) were used as a benchmark for comparison between tag design performances. A substrate with values at the centre of the testing

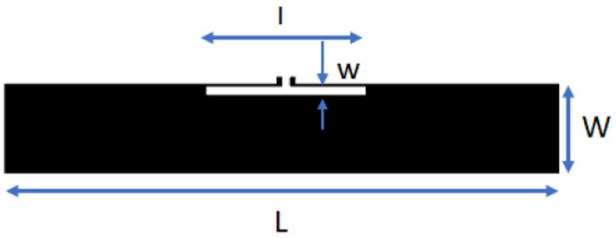

Fig. 2 Slot antenna geometry

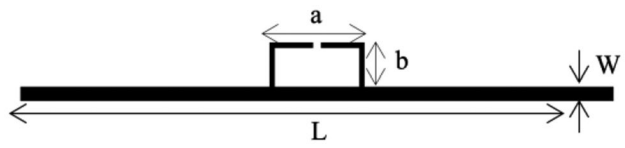

Fig. 3 T-match dipole antenna geometry

Table 2 Dimensions of T-matched dipole RFID tags for S11 < − 15 dB

Antenna name	*W* (mm)	*L* (mm)	*a* (mm)	*b* (mm)
Dipole: $\varepsilon_r = 3$, $t = 6$ mm	3.46	144	23	11.15
Dipole: $\varepsilon_r = 3$, $t = 6$ mm ***M***	3.46	115	19	41.15

range (i.e. $\varepsilon_r = 3$ and $t = 6$ mm) was used in the "benchmark" designs. Two T-match antenna designs were created, one that was impedance matched for location MP and the other for NMP. The impedance matching for these tags was achieved by adjusting the length of the antenna (L) and the parameters of the T part of the antenna (i.e. lengths a and b in Fig. 3). The parameters for these tags are listed in Table 2. To compare the performance of the designed tags to a commercially available tag, the Alien Squiggle RFID tag [21] was simulated using the same parameters.

2.1.2 Effective permittivity values for each simulation setup

The effective permittivity helps to determine the length of antenna required to obtain resonance at the required frequency (i.e. 868 MHz for UHF RFID systems); see Eqs. (1)–(3). The calculated effective permittivities are listed in Table 3. Equation (1) was used for the NMP simulations which are unaffected by substrate thickness, so the value for each effective permittivity is only calculated once. Equations (2) and (3) were used for the MP simulations which include the thickness of the substrate, so the calculations were repeated for all the required combinations of ε_r (i.e. 1, 3, 5) and thicknesses (i.e. 0.5 mm, 1 mm, 2 mm, 4 mm, 6 mm, 8 mm and 10 mm).

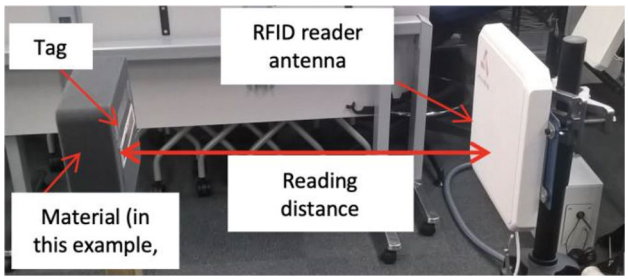

Fig. 4 Measurement setup with RFID tags on foam

2.1.3 Simulations on substrates for MP and NMP scenarios

Each antenna design was simulated on different substrates with different thicknesses. For each simulation, the radiation efficiency, total efficiency and *gain* were recorded. The radiation efficiency is the ratio of the amount of power that the antenna radiates to the amount of power that is accepted at its terminals. The total efficiency is the ratio of the amount of power that is radiated to the amount of power put into the antenna and includes the mismatch loss. The gain is the amount of power that is transmitted in the direction of peak radiation compared to that of an isotropic radiator with the same input power. The goal is to get the efficiency values close to 100%. A higher gain value results in a higher read range of the tag. Each tag simulation was run 35 times, and an average was taken to yield the results given below.

2.2 Physical read range testing

The location of the RFID reader antenna (RFID-RA) [25] was fixed, and the read performance was measured as the average received signal strength indicator (RSSI) over 50 reads at each location. Reads were taken from 0.5 to 6 m using 0.5-m intervals. The test setup is shown in Figs. 4 and 5. Polyurethane foam (230 mm × 175 mm × 70 mm) backing was used in all testing to physically support the tag without affecting the EM behaviour with $\varepsilon_r = 1.04$, similar to that of air [26]. The Dipole, Slot and Alien Squiggle antenna designs from the simulations were etched onto Rogers RO3003 material

Table 3 Effective permittivity for different simulation setups for all antennas

Substrate permittivity ε_r	NMP	Substrate thickness (mm) MP						
		0.5	1	2	4	6	8	10
1	1.0	1.0	1.0	1.0	1.0	1.0	1.0	1.0
2	1.5	1.9	1.9	1.8	1.8	1.7	1.7	1.7
3	2.0	2.9	2.8	2.7	2.5	2.5	2.4	2.4
4	2.5	3.8	3.7	3.5	3.3	3.2	3.1	3.1
5	3.0	4.8	4.6	4.4	4.1	3.9	3.8	3.8

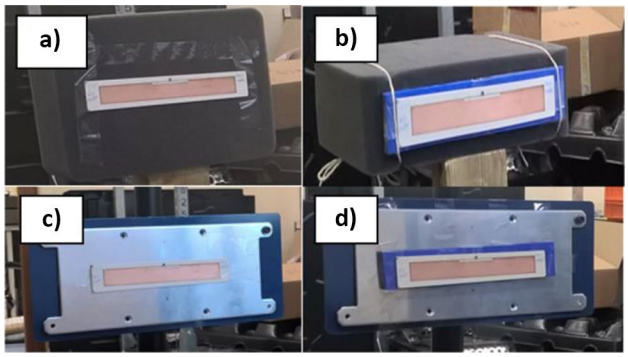

Fig. 5 Read range measurement setup **a** on polyurethane foam, **b** on silicone, **c** MP and **d** on silicone with MP

which has a dielectric constant of 3 (+/−0.04) and a loss tangent of 0.0013 at 10 GHz [27]. The thickness of the dielectric material was 1.52+/−0.08 mm with a copper cladding of 35.00+/−0.05 µm. The RFID chip used for all the tag antennas was the Alien Higgs 3 SOT.

For the first test, the tags were located on. In the second test, each tag was attached to an aluminium plate (255 mm×120 mm×3 mm). To investigate the effects of a dielectric material on performance, the three tags were placed onto a 10-mm thick silicone separator with ε_r=2.9 [28]. The final experiment was used to determine the effect of dielectric spacers on read range performance, evaluated by attaching the tags to the silicone spacer on a metal plate. The read performance of each of the tag designs was measured in the four described measurement test setups, as shown in Fig. 5.

3 Results and discussion

3.1 Results of the simulations

A summary of results for the different combinations of tag designs is summarised in Tables 4 (MP) and 5 (NMP). The average radiation efficiency (16.0 to 60.2%, SD=18.0 to 39.0) is lower for all the tags with MP than NMP (78.4 to 97.2%, SD=1.3 to 14.8). This is the result of a wider variation in the effective permittivity of the substrate with the MP simulations (see Table 3). The commercial *Alien Squiggle* tag had greater radiation efficiency when there was NMP (i.e. 16.0%, SD=18.0 MP compared with 91.3%, SD=6.9 NMP).

The total efficiency results are presented in Tables 6 (NMP) and 7 (MP). In the NMP scenarios, the tags designed for NMP performance had a better total efficiency (e.g. 30.5 to 76.1%, SD=11.4 to 22.8) than the tags designed to work MP (e.g. 1.2 to 3.6%, SD=1.0 to 2.5). However, on inspection of the MP results, the antennas designed for MP show a lower average total efficiency (1.8 to 11.2%, SD=4.1 to 22.6) than for the tags designed for NMP (10.2 to 15.4%, SD=11.3 to 17.2). Table 7 also indicates, in the worst case, all tags yield a total efficiency of near zero; i.e. they do not radiate at all when placed MP.

The average gain values were lower for all tags in the simulations for MP scenarios (−24.5 to −9.0 dBi, SD=8.5 to 15.0) compared with NMP designs (−19.9 to 0.9 dBi, SD=0.6–3.8) quantifying the significant effect of the metal on antenna gain. The highest gain values were for the tags slot: ε_r=5, t=10 mm M (2.6 dBi) and slot: ε_r=5, t=10 mm (2.3 dBi) for MP trials, showing that the presence of metal can help increase the gain. Nonetheless, the tags designed for NMP showed lower variations (SD=0.7 to 11.9) and higher average (average gain=−13.0 to 0.9 dBi) compared with tags designed for MP applications (average gain=−22.0 to −12.3 dBi, SD=0.6–15.0), implying that the NMP tags may be more robust choices for a variety of different materials.

3.1.1 Efficiency variation for tags on different substrates with NMP

The commercial tag was evaluated with total efficiency simulation results presented in Fig. 6a. Inspection of the results indicates the tag works well for all materials however reduces its effectiveness as the substrate thickness increases,

Table 4 Simulated radiation and total efficiencies (%) results for RFID tags on different substrates (NMP)

Tag name	Radiation efficiency (total efficiency %)			
	Max	Min	Average	Standard deviation
Squiggle	97.5 (96.8)	71.2 (15.3)	91.3 (48.5)	6.9 (25.9)
Dipole: ε_r=3, t=6 mm	97.3 (94.9)	91.1 (53.0)	95.5 (72.9)	1.7 (14.3)
Slot: ε_r=1, t=2 mm	96.0 (91.8)	86.1 (41.4)	93.0 (77.0)	2.7 (15.0)
Slot: ε_r=3, t=6 mm	94.4 (92.5)	90.1 (58.1)	92.5 (76.1)	1.3 (11.4)
Slot: ε_r=5, t=10 mm	91.4 (83.9)	72.3 (7.4)	80.0 (30.5)	5.4 (22.8)
Dipole: ε_r=3, t=6 mm ***M***	94.7 (8.6)	67.9 (0.8)	84.0 (3.0)	8.8 (2.5)
Slot: ε_r=1, t=2 mm ***M***	99.7 (4.5)	95.6 (2.8)	99.5 (3.6)	1.3 (0.5)
Slot: ε_r=3, t=6 mm ***M***	99.8 (9.3)	87.2 (0.6)	97.2 (2.2)	3.8 (2.1)
Slot: ε_r=5, t=10 mm ***M***	99.7 (4.8)	53.5 (0.4)	78.4 (1.2)	14.8 (1.0)

Table 5 Simulated radiation and total efficiencies (%) results for RFID tags on different substrates (MP)

Tag name	Radiation efficiency (total efficiency)			
	Max	Min	Average	Standard deviation
Squiggle	62.8 (7.6)	0.0 (0.0)	16.0 (1.9)	18.0 (2.2)
Dipole: $\varepsilon_r = 3$, $t = 6$ mm	81.2 (45.7)	0.6 (0.0)	41.2 (10.2)	27.3 (12.6)
Slot: $\varepsilon_r = 1$, $t = 2$ mm	80.6 (38.7)	0.9 (0.0)	42.5 (12.4)	25.2 (11.3)
Slot: $\varepsilon_r = 3$, $t = 6$ mm	87.2 (45.2)	0.4 (0.0)	47.6 (15.4)	30.4 (16.4)
Slot: $\varepsilon_r = 5$, $t = 10$ mm	90.3 (63.4)	1.6 (0.0)	47.3 (13.8)	31.7 (17.2)
Dipole: $\varepsilon_r = 3$, $t = 6$ mm ***M***	78.9 (34.5)	0.1 (0.0)	25.5 (4.9)	24.6 (11.1)
Slot: $\varepsilon_r = 1$, $t = 2$ mm ***M***	99.5 (19.5)	1.5 (0.0)	60.2 (1.8)	39.0 (4.1)
Slot: $\varepsilon_r = 3$, $t = 6$ mm ***M***	94.2 (50.4)	0.2 (0.0)	57.1 (7.6)	33.5 (13.8)
Slot: $\varepsilon_r = 5$, $t = 10$ mm ***M***	99.5 (75.6)	0.3 (0.0)	42.1 (11.2)	30.8 (22.6)

with the lowest total efficiency (15.3%) on a 10-mm substrate. The simulation also suggests this tag is best suited to a substrate with $\varepsilon_r = 2$ (e.g. polytetrafluoroethylene (PTFE) [29] as this yields higher efficiencies for all material thicknesses (max 95.3% at 2 mm). The total efficiency results of the dipole tag are presented in Fig. 6b, showing an improved range of functionality when compared with the squiggle tag, for larger substrate thicknesses and higher permittivities. The efficiency was greater than 53% for all simulations. The tag performed best on materials within its design criteria (i.e. rubber (hard) [30]). The read range results for the three slot tags NMP operation are detailed in Fig. 6c–e. As with the dipole design, each slot design had the largest total efficiency at the values that the tags were designed for. All the simulations for Slot: $\varepsilon_r = 1$, $t = 2$ mm had a total efficiency greater than 41.4% and Slot: $\varepsilon_r = 3$, $t = 6$ mm had a total efficiency greater than 58.1% for all simulations showing good all-round performance for many materials and thicknesses. The slot designed for the extreme case, $\varepsilon_r = 5$ (e.g. glass Pyrex [31]) and $t = 10$ mm performed poorly in general and with a maximum efficiency of 56% (at $\varepsilon_r = 5$ with a 4-mm substrate), showing poor performance for any likely uses in industry for NMP scenarios.

With the exclusion of the slot εr = 5, $t = 10$ mm, the designed tags perform well over a wide range of substrate materials and thicknesses for use in industry where the tag is to be positioned for NMP scenarios. The simulated tags can also be seen to outperform the squiggle tag for much of the target permittivities and substrates.

3.1.2 Total efficiency results for tags designed to work MP in an NMP scenario

The tags specifically designed for MP operation performed poorly in all NMP scenarios. The simulated total efficiency results for Dipole: $\varepsilon_r = 3$, $t = 6$ mm M when there is no ground plane for example (Fig. 6f) yields the highest total efficiency of 8.6% on a substrate with a ε_r of 4-mm and 10-mm thick, significantly lower than for the tag designed for NMP (0.8 to 8.6% compared with 53 to 95%).

The results for the three slot tags designed to work MP (Fig. 6g–i) were similar to the dipole yielding maximum efficiencies of 4.5% for Slot $\varepsilon_r = 1$, $t = 2$ mm M, 9.3% for Slot: $\varepsilon_r = 3$, $t = 6$ mm M and 4.8% for Slot: $\varepsilon_r = 5$, $t = 10$ mm M. The trend throughout the simulations was an increase in

Table 6 Simulated total gain (dBi) results for RFID tags on substrates (NMP)

Tag name	Max	Min	Average	Standard deviation
Squiggle	1.8	−6.0	−1.8	2.4
Dipole: $\varepsilon_r = 3$, $t = 6$ mm	1.9	−0.7	0.6	0.9
Slot: $\varepsilon_r = 1$, $t = 2$ mm	1.7	−1.7	0.9	0.9
Slot: $\varepsilon_r = 3$, $t = 6$ mm	1.7	−0.5	0.7	0.7
Slot: $\varepsilon_r = 5$, $t = 10$ mm	1.2	−9.9	−4.8	3.6
Dipole: $\varepsilon_r = 3$, $t = 6$ mm ***M***	−8.6	−19.8	−15.1	3.8
Slot: $\varepsilon_r = 1$, $t = 2$ mm ***M***	−11.3	−13.4	−12.3	0.6
Slot: $\varepsilon_r = 3$, $t = 6$ mm ***M***	−8.3	−21.3	−16.7	3.8
Slot: $\varepsilon_r = 5$, $t = 10$ mm ***M***	−11.6	−24.4	−19.9	3.7

Table 7 Simulated total gain (dBi) results for RFID tags on different substrates (MP)

Tag name	Max	Min	Average	Standard deviation
Squiggle	−4.2	−52.3	−24.5	14.7
Dipole: $\varepsilon_r = 3$,$t = 6$ mm	1.1	−41.3	−13.0	11.4
Slot: $\varepsilon_r = 1$,$t = 2$ mm	0.6	−28.5	−9.0	8.5
Slot: $\varepsilon_r = 3$,$t = 6$ mm	1.4	−41.2	−10.4	10.6
Slot: $\varepsilon_r = 5$,$t = 10$ mm	2.3	−46.0	−12.3	11.9
Dipole: $\varepsilon_r = 3$,$t = 6$ mm ***M***	−0.1	−40.7	−22.0	11.7
Slot: $\varepsilon_r = 1$,$t = 2$ mm ***M***	0.0	−36.0	−20.2	9.3
Slot: $\varepsilon_r = 3$,$t = 6$ mm ***M***	1.1	−51.5	−18.6	13.5
Slot: $\varepsilon_r = 5$,$t = 10$ mm ***M***	2.6	−50.7	−21.1	15.0

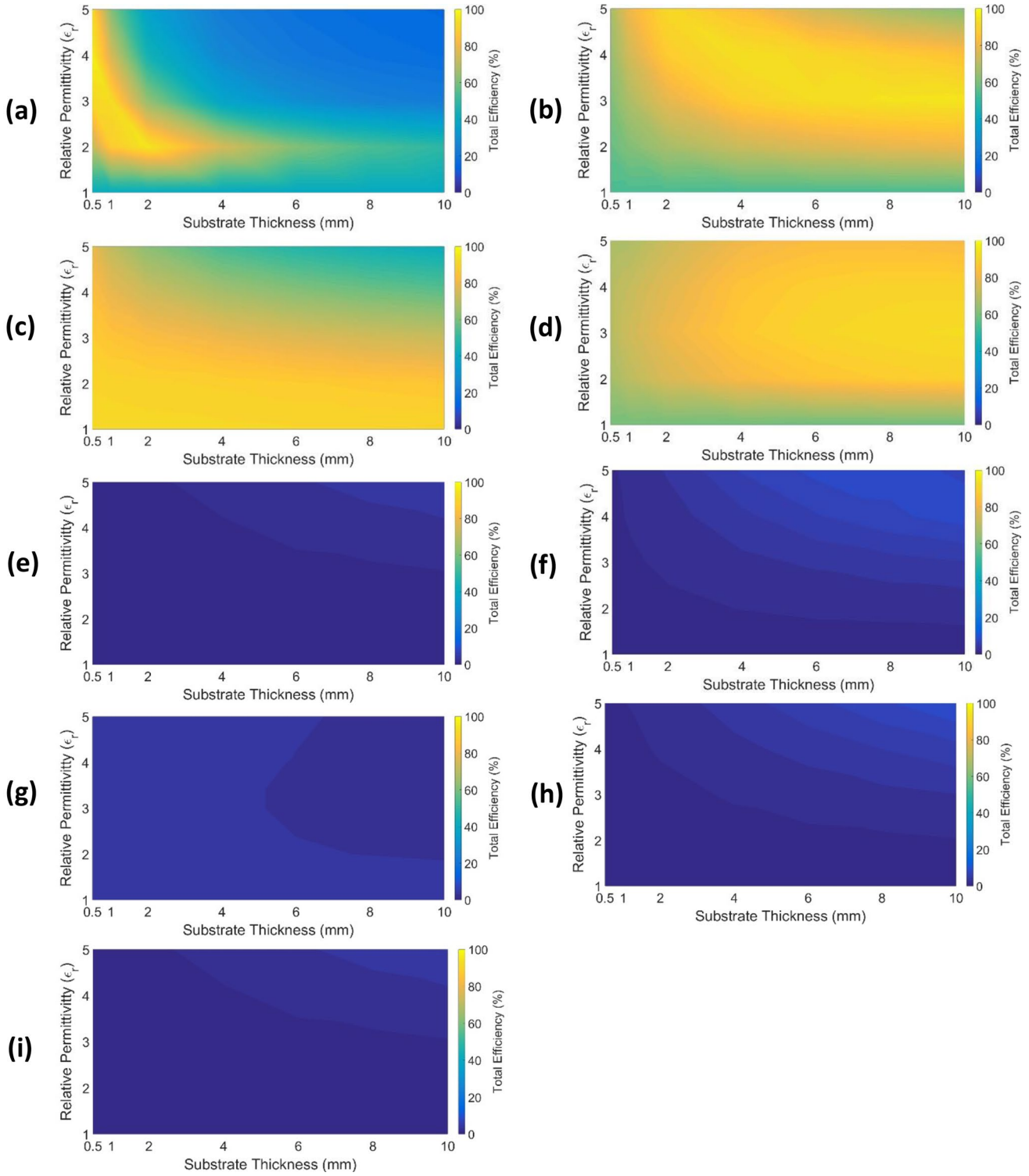

Fig. 6 Total efficiency results for the 9 tag designs on a variety of dielectrics with NMP. Reading left to right: **a** Squiggle, **b** Dipole: $\varepsilon_r = 3$, $t = 6$ mm, **c** Slot: $\varepsilon_r = 1$, $t = 2$ mm, **d** Slot: $\varepsilon_r = 3$, $t = 6$ mm, **e** Slot: $\varepsilon_r = 5$, $t = 10$ mm, **f** Dipole: $\varepsilon_r = 3$, $t = 6$ mm M, **g** Slot: $\varepsilon_r = 1$, $t = 2$ mm M, **h** Slot: $\varepsilon_r = 3$, $t = 6$ mm M, **i** Slot: $\varepsilon_r = 5$, $t = 10$ mm M

efficiency with either an increase in permittivity (e.g. 0.6% at $\varepsilon_r = 1$ to 5.7% at $\varepsilon_r = 5$ when on a 6-mm thick substrate) or an increase in thickness (e.g. 0.8% at 0.5-mm thick to 3.1% at 10-mm thick on a substrate with a ε_r of 3).

It is noted that the increase in permittivity results in higher efficiency values as the effective permittivity approaches the permittivity the tag was designed for. However, all tags designed to work with MP were an order of magnitude less efficient than those designed for NMP in NMP conditions.

3.1.3 Simulated total efficiency for tags designed for NMP in an MP scenario

The simulation results for the total efficiency values of the tags, designed to work with NMP, with variance of the set of substrate parameters (e.g. $\varepsilon_r = 1$ to 5, thickness = 0.5 to 10 mm) used previously but with a rectangular piece of metal (160 × 30 × 1 mm) below each tag are given in Fig. 7. The substrate is sandwiched between the tag and metal, so the substrate thickness represents the distance between the antenna and metal. These sets of results were undertaken to determine how well tags that are designed for applications with NMP can perform with MP and how thick a substrate is required for the tags to work robustly and reliably.

The commercial *Alien Squiggle* tag is not described as being able to work when placed MP [21], and hence, it was adopted as a benchmark of performance for these simulations. The total efficiency for the *Alien Squiggle* tag above metal derived from the simulations can be seen in Fig. 7a. This tag does not respond when located 0.5 mm from the metal with any of the ε_r values. The efficiency improves as the thickness of the dielectric is increased with the largest efficiency of 7.6% achieved when the thickness is 10 mm and the ε_r is 1, similar to the values seen when a tag designed for MP conditions was located with NMP.

The tags designed to work with NMP showed more leniency than the squiggle tag, with the dipole tag (Fig. 7b) yielding a maximum total efficiency of 45.7% ($\varepsilon_r = 3$ and the thickness = 10 mm). It is noted, however, in close proximity, the efficiency is drastically reduced, less than 0.5% when the tag is 0.5 mm or 1 mm away from the metal. The total efficiency for the *dipole* tag shows an increase as the thickness of the substrate is increased (i.e. average increase of 25% for all 5 permittivities) with maximum values occurring at its design point $\varepsilon_r = 3$. For demonstration, the effect of permittivity can be seen to peak at $\varepsilon_r = 3$ thickness = 8 mm with total efficiency values of 1.4%, 16.8%, 36.2%, 31.6% and 18.9% for the permittivities of 1, 2, 3, 4 and 5, respectively.

The simulated total efficiency results for the designed slot tags Fig. 7c–e. All three tags show an increase in efficiency with an increase in substrate thickness (i.e. for Slot: $\varepsilon_r = 3$, $t = 6$ mm on substrate with ε_r of 3 the efficiency changes from 0.1% on 0.5-mm substrate to 42.4% on 10-mm substrate) as the tags are moved further from the detuning effects of the metal. The slot tags also perform better the higher their designed ε_r with maximum efficiency values of 10.5% for Slot: $\varepsilon_r = 1$, $t = 2$ mm, 45.2% for Slot: $\varepsilon_r = 3$, $t = 6$ mm and 63% for Slot: $\varepsilon_r = 5$, $t = 10$ mm. However, unlike the dipole tag, the maximal performance of each tag does not coincide with its design point when in an MP condition.

In general, all designed tags outperformed the squiggle tag in the MP scenario, and at low permittivity and low substrate thickness, all tags yield the worst efficiency.

3.1.4 Simulated total efficiency results for tags designed to work with MP in an MP scenario

The simulated total efficiency results for the tags designed to work with MP in the MP scenario can be seen in Fig. 7f–i. The maximum total efficiency for the dipole was 34.5% and occurred at its design parameters. The tag had an efficiency greater than 25% for all simulations when the ε_r was 3, excluding close proximity to the metal with substrate thicknesses of 0.5 mm and 1 mm (efficiencies of 0.6% and 3.4%, respectively). The total efficiency was greatly reduced for all the other permittivities; e.g. for ε_r of 5, the average efficiency for all thicknesses was 0.2%, showing a high performance at the design point but little flexibility around this.

The simulated total efficiency results for the *slot* tags designed to work MP, presented in Fig. 7g–i, respectively, show a similar trend with each of the tags yielding the largest efficiency when the permittivities were equal to the designed values; however, they showed more flexibility than the dipole tag. All three of the Slot tags showed a greater reduction in total efficiency as the permittivity value changed from the designed value; e.g. for Slot: $\varepsilon_r = 3$, $t = 6$ mm M, the average efficiency on a substrate with a value of 3 was 30.2%, whereas for permittivity of 4, it was 4.5%, and permittivity of 5, it was 2.4%.

The largest total efficiency for each slot tag were 19.5%, 50.4% and 75.6% for Slot: $\varepsilon_r = 1$, $t = 2$ mm M, Slot: $\varepsilon_r = 3$, $t = 6$ mm M and Slot: $\varepsilon_r = 5$, $t = 10$ mm M, respectively. These results demonstrate the increases in total efficiency that can be achieved with higher permittivity substrates and that performance of designed tags for MP adhere well to their design point.

In general, none of the tags designed to work with MP worked well in close proximity < 0.5 mm from the metal ground plane. The tags designed to perform with MP also strongly adhere to their design point with a significant reduction in efficiency upon straying from the design ε_r. In addition, it appears the deviation from the ε_r has a much greater impact on efficiency than the deviation from the designed substrate thickness when the thickness is > 1 mm.

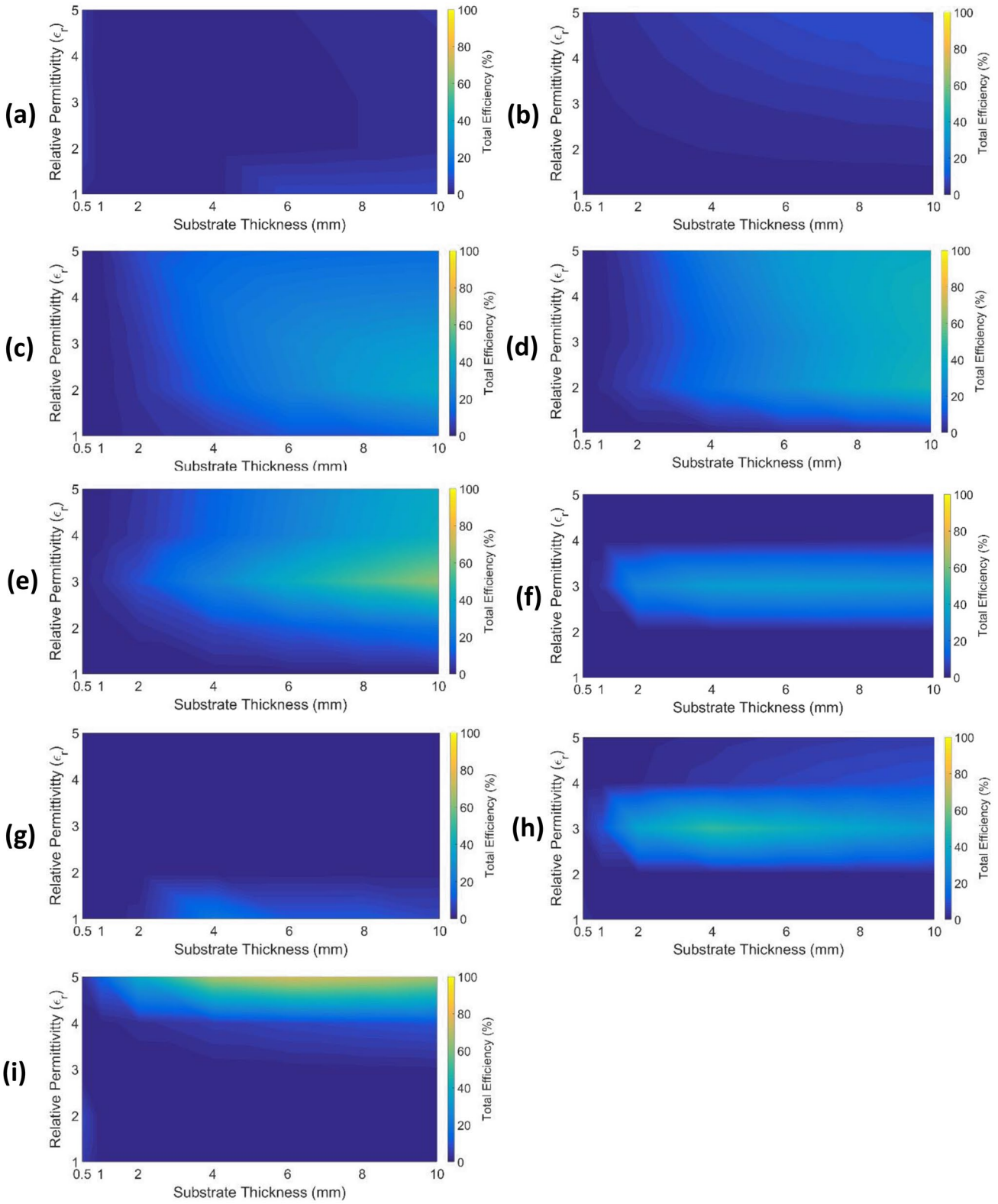

Fig. 7 Total efficiency results for the 9 tag designs with MP Reading left to right: **a** Squiggle, **b** Dipole: $\varepsilon_r = 3$, $t = 6$ mm, **c** Slot: $\varepsilon_r = 1$, $t = 2$ mm, **d** Slot: $\varepsilon_r = 3$, $t = 6$ mm, **e** Slot: $\varepsilon_r = 5$, $t = 10$ mm, **f** Dipole: $\varepsilon_r = 3$, $t = 6$ mm M, **g** Slot: $\varepsilon_r = 1$, $t = 2$ mm M, **h** Slot: $\varepsilon_r = 3$, $t = 6$ mm M, **i** Slot: $\varepsilon_r = 5$, $t = 10$ mm M

3.2 Read range simulation results

3.2.1 Summary of simulated read range results MP testing

A summary of the simulation results for the performance of the tags designed for MP and designed for NMP when located with MP is presented in Table 8. The results indicate the Dipole and Slot tags performed better (i.e. larger read ranges) than the Alien Squiggle tag in the MP scenario. In addition, the maximum predicted read ranges for the tags designed to work MP (e.g. Slot: $\varepsilon_r = 3$, $t = 6$ mm M, max read range of 11.1 m) were similar to the tags *not* designed to work MP (e.g. Slot: $\varepsilon_r = 3$, $t = 6$ mm, max read range of 11.5 m) when both types of tags were simulated in MP conditions. However, the average read ranges for the NMP-designed tags (average read range between 4 and 4.9 m) were higher than the MP-designed tags (average read range between 1.8 and 2.9 m). This shows that the NMP-designed tags are more robust in the MP conditions than the MP-designed tags, once again contradicting the hypothesis.

3.2.2 Summary of simulated read range results for tags in NMP testing

A summary of the simulation results for tag performance when located on different dielectrics with NMP is detailed in Table 9. The table contains an average read range for each tag for all the simulated combinations of ε_r values (1 to 5) and thicknesses (0.5 to 10 mm). The table also includes the maximum predicted read range for each tag and the percentage of results that were either above 6 m or below 1 m. A comparison of the NMP read ranges with the equivalent MP results shows that all the NMP tags perform better (i.e. average increase in read range of 7.9 m) than the tags that were designed to be in MP conditions. The anomaly in the NMP performance is the slot tag designed for a ε_r of 5, Slot: $\varepsilon_r = 5$, $t = 10$ mm as its average read range was 4.6 + / − 0.2 m, lower than the other NMP tags. This indicates that the design of this tag with a high ε_r and thickness was less robust to being located on the different simulated substrates than the other NMP tag designs.

3.3 Results of the physical test for RSSI read range

The results of the experiment for the physical tags when they were attached to foam support are presented in Fig. 8. The tag with the largest read range was the Alien Squiggle tag which was read at the maximum distance possible in the laboratory of 6 m. This is expected as this tag should have been able to be read at greater than 10 m from the simulations. The Dipole and Slot tags were predominantly readable up to 4 m distances from the RFID-RA except for the Slot: $\varepsilon_r = 5$, $t = 10$ mm M which read up to 1 m and the Dipole: $\varepsilon_r = 3$, $t = 6$ mm M which only read up to 0.5 m. It is interesting to note that the manufactured Slot tags did not achieve the same read ranges as the commercial Alien Squiggle tag since the simulations indicated that the Slot tags would achieve a higher read range when on the permittivity of 1. Furthermore, the two tags that were only read at distances < 1 m were designed for operation with MP, and in the first set of trials (Fig. 8), the tests were conducted in NMP conditions.

The results when using the manufactured tags on silicone are represented in Fig. 9. The largest read range was observed for the Alien Squiggle tag at 6 m. The shortest read range was obtained from the Dipole: $\varepsilon_r = 3$, $t = 6$ mm M tag at only 0.5 m, followed by the Slot: $\varepsilon_r = 5$, $t = 10$ mm at 1.5 m. All the remaining tag designs resulted in an average read ranges of 4 m. It is noted that there is little difference between the silicone substrate results and the foam substrate results for most of the tags (i.e. only the Slot: $\varepsilon_r = 5$, $t = 10$ mm tag showed a different read range on the different materials). This is likely due to only the permittivity of the material the tag is attached to being changed in the measurement setup (i.e. $\varepsilon_r = 1$ for foam and $\varepsilon_r = 2.9$ for silicone). This mirrors the results observed in the simulations in Sect. 3, which showed very little change in the predicted read range for different ε_r values (i.e. the average change

Table 8 Summary of simulation results for RFID tags on different dielectrics (MP)

Antenna name	Average read range (m)	Max read range (m)	Percentage above 6-m read range	Percentage below 1-m read range
Squiggle	1.4	6.0	5.7	45.7
Dipole: $\varepsilon_r = 3$, $t = 6$ mm	4.0	11.1	31.4	28.6
Slot: $\varepsilon_r = 1$, $t = 2$ mm	4.9	10.5	45.7	14.3
Slot: $\varepsilon_r = 3$, $t = 6$ mm	4.9	11.5	42.9	17.1
Slot: $\varepsilon_r = 5$, $t = 10$ mm	4.5	12.7	34.3	28.6
Dipole: $\varepsilon_r = 3$, $t = 6$ mm ***M***	2.0	9.7	14.3	60.0
Slot: $\varepsilon_r = 1$, $t = 2$ mm ***M***	1.8	9.8	11.4	45.7
Slot: $\varepsilon_r = 3$, $t = 6$ mm ***M***	2.8	11.1	14.3	42.9
Slot: $\varepsilon_r = 5$, $t = 10$ mm ***M***	2.9	13.2	14.3	51.4

Table 9 Summary of simulation results for RFID tags on different dielectrics (NMP)

Antenna name	Average read range (m)	Max read range (m)	Percentage above 6-m read range	Percentage below 1-m read range
Squiggle	8.3	12.0	77.1	0
Dipole: $\varepsilon_r = 3$, $t = 6$ mm	10.6	12.2	100	0
Slot: $\varepsilon_r = 1$, $t = 2$ mm	10.9	11.9	100	0
Slot: $\varepsilon_r = 3$, $t = 6$ mm	10.7	11.9	100	0
Slot: $\varepsilon_r = 5$, $t = 10$ mm	6.1	11.2	42.9	0
Dipole: $\varepsilon_r = 3$, $t = 6$ mm ***M***	1.9	3.6	0	0
Slot: $\varepsilon_r = 1$, $t = 2$ mm ***M***	2.4	2.7	0	0
Slot: $\varepsilon_r = 3$, $t = 6$ mm ***M***	1.6	3.8	0	22.9
Slot: $\varepsilon_r = 5$, $t = 10$ mm ***M***	1.1	2.6	0	57.1

in the predicted read range for the designed tags over all ε_r was 2.6 m).

The results for the tags when attached to the metal plate are presented in Fig. 10. The tags that were read were Slot: $\varepsilon_r = 1$, $t = 2$ mm up to 4.5 m, Slot: $\varepsilon_r = 3$, $t = 6$ mm up to 2 m, Dipole: $\varepsilon_r = 3$, $t = 6$ mm up to 1 m and Slot: $\varepsilon_r = 5$, $t = 10$ mm up to 0.5 m. This outcome was unexpected as the tags that were designed for NMP outperformed the tags that were designed for operation for MP, further contradicting the hypothesis. For example, Slot: $\varepsilon_r = 3$, $t = 6$ mm designed for NMP operation outperformed the Slot: $\varepsilon_r = 3$, $t = 6$ mm M its MP counterpart which did not read with a read range of 2 m. In addition, the tag that was designed to perform best on the thinnest substrate Slot: $\varepsilon_r = 1$, $t = 2$ mm (i.e. 2-mm thick substrate) was the one that achieved the largest read range of 4.5 m. This result is because there was only a small separation of 1.52 mm +/− 0.08 mm between the tags and the metal surface due to the thin substrate that the antennas were printed on. This phenomenon could be partially due to tolerances in manufacturing for each tag, for example, variations in the tag printing, microchip soldering and substrate thickness which all impact tag readability. Furthermore, the simulation suggested that all tags in regions very close to metal performed poorly; however, the simulation does not account for additional reflections and multipath influences that may occur within a room. Further work will be required to understand why the tags designed to work in NMP conditions did not perform in accordance with the simulated scenario.

The final sets of results are for the tags located MP, with a 10-mm silicone spacer between, as presented in Fig. 11. The largest read range observed was 4.5 m achieved by the Slot: $\varepsilon_r = 3$, $t = 6$ mm, and the shortest was 0.5 m by Dipole: $\varepsilon_r = 3$, $t = 6$ mm M. Two tags achieved a read range of 4 m, the Slot:

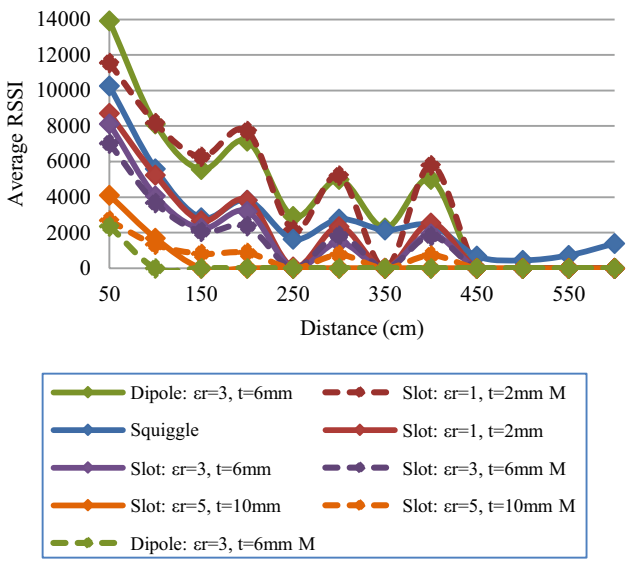

Fig. 8 Measurement results with RFID tags on foam (The legend is ordered as per the highest average RSSI at 50 cm)

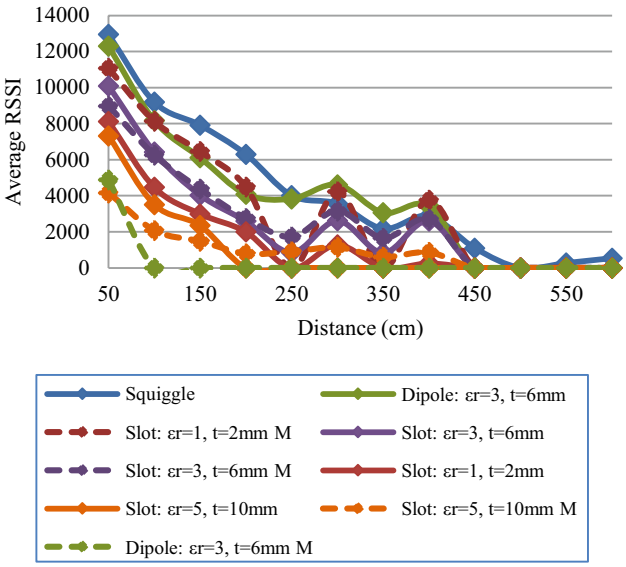

Fig. 9 Measurement results of RFID tags on 10-mm thick silicone (The legend is ordered as per the highest average RSSI at 50 cm)

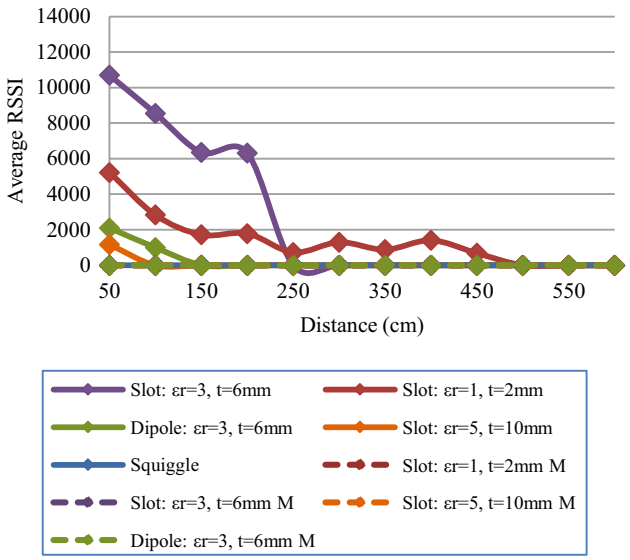

Fig. 10 Measurement results with RFID tags 1.52 mm from metal (i.e. only the Rogers RO3003 material). The legend is ordered as per the highest average RSSI at 50 cm. Note: only 4 tags could be read

$\varepsilon_r = 3$, $t = 6$ mm M and the Dipole: $\varepsilon_r = 3$, $t = 6$ mm. The Slot: $\varepsilon_r = 1$, $t = 2$ mm, Squiggle and Slot: $\varepsilon_r = 5$, $t = 10$ mm M tags achieved a read range of 2 m. Finally, the Slot: $\varepsilon_r = 5$, $t = 10$ mm and the Slot: $\varepsilon_r = 1$, $t = 2$ mm M a 1.5 m and 1 m read range, respectively.

All the tags except the Slot: $\varepsilon_r = 1$, $t = 2$ mm showed an increase in read range (average increase = 2.1 m +/− 1.9 m)

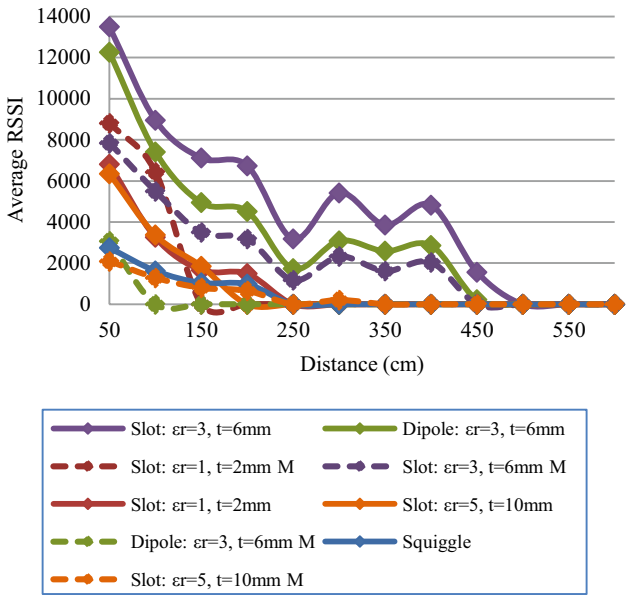

Fig. 11 Measurement results of RFID tags MP with 10-mm silicone spacer (The legend is ordered as per the highest average RSSI at 50 cm)

when the silicone spacer was added when compared with a direct attachment to the metal. The Slot: $\varepsilon_r = 1$, $t = 2$ mm tag's read range decreased from 4.5 m (directly MP) to 2 m (MP with silicone spacer). The situation is complicated, however, since the Slot: $\varepsilon_r = 1$, $t = 2$ mm tag did show an increase in RSSI when measured at 0.5 m, with a value of 5225 MP and 6807 when MP and silicone. This is most likely due to the fact that when the tag was located on the silicone spacer and metal, the effective permittivity was higher (i.e. $\varepsilon_r = 2.38$) than the value that this tag was designed for (i.e. $\varepsilon_r = 1$). For the Slot tags designed with relative permittivities of 3 and the dipole tag, it was the NMP-designed versions of the tags (Slot: $\varepsilon_r = 3$, $t = 6$ mm and Dipole: $\varepsilon_r = 3$, $t = 6$ mm) that outperformed the ones designed for MP operation (Slot: $\varepsilon_r = 3$, $t = 6$ mm M and Dipole: $\varepsilon_r = 3$, $t = 6$ mm). This result perhaps indicates how these tag designs may be more robust than their MP-designed counterparts. However, with the Slot tags on the permittivity of 5, it was the MP-designed tag Slot: $\varepsilon_r = 5$, $t = 10$ mm M that performed better than the NMP equivalent Slot: $\varepsilon_r = 5$, $t = 10$ mm with read ranges of 3 m and 1.5 m, respectively. It should be noted that experimental conditions for this slot tag were closest to its design parameters (i.e. on a 10-mm substrate above metal) as the experiments were performed with a 10-mm silicone substrate.

3.4 Discussion of read range measurement results

The RSSI values fluctuated as the distance between tag and reader was increased. This behaviour would not be expected if the experiments were to be undertaken in free space (or in an anechoic chamber), as the RSSI should decrease steadily with an increasing distance [32]. However, these measurements were carried out in a laboratory, so reflections of the signal from the floor, walls and any objects within the room will influence the results. Reflections result in multiple delayed multipath signals arriving at the RFID-RA simultaneously which can cause significant fluctuations in RSSI (as noted in [33–35]). To aid comparison, an average of the measured RSSI's for each tag in each test setup is shown in Table 10.

The largest average RSSI on the foam was the Dipole: $\varepsilon_r = 3$, $t = 6$ mm (RSSI = 4160), followed by the Slot: $\varepsilon_r = 1$, $t = 2$ mm M tag (RSSI = 3908). The Dipole: $\varepsilon_r = 3$, $t = 6$ mm tag was specifically designed for the Rogers RO3003 substrate the antennas were printed on, and therefore, the higher performance is as expected. However, the performance of the Slot: $\varepsilon_r = 1$, $t = 2$ mm M was unusual as it was designed to operate MP. The highest average RSSI recorded on the 10-mm silicone substrate was the Alien Squiggle tag (RSSI = 4241) with the Dipole: $\varepsilon_r = 3$, $t = 6$ mm the second highest (RSSI = 3800). When attached directly to the metal, the Slot: $\varepsilon_r = 3$, $t = 6$ mm had the highest average

Table 10 Average RSSI for all measurements of each RFID tag

Antenna name	Foam	Metal (RO3003)	Silicone	Silicone + metal
Squiggle	2892	0	4241	532
Slot: $\varepsilon_r = 1$, $t = 2$ mm	2117	1378	1592	1101
Slot: $\varepsilon_r = 3$, $t = 6$ mm	1751	2659	2504	4596
Slot: $\varepsilon_r = 5$, $t = 10$ mm	483	97	1099	964
Dipole: $\varepsilon_r = 3$, $t = 6$ mm	4160	259	3800	3302
Slot: $\varepsilon_r = 1$, $t = 2$ mm ***M***	3908	0	3180	1269
Slot: $\varepsilon_r = 3$, $t = 6$ mm ***M***	1563	0	2632	2264
Slot: $\varepsilon_r = 5$, $t = 10$ mm ***M***	598	0	1002	420
Dipole: $\varepsilon_r = 3$, $t = 6$ mm ***M***	197	0	406	255

RSSI = 2659, and the Slot: $\varepsilon_r = 1$, $t = 2$ mm had the second highest RSSI = 1378. That none of the tags, designed for operation MP, worked when they were attached directly to the metal, is perhaps not surprising as they were designed with a larger separation than the substrate thickness. Nevertheless, all the tags had a larger average RSSI with the silicone spacer (overall RSSI average = 2273) than when directly on the metal (overall RSSI average = 488). As expected, the dielectric spacer reduced the effects of the metal on the RFID tag impedance mismatch.

In terms of the total average RSSI performance for each of the designed tags, the tags with the highest RSSI were the Slot: $\varepsilon_r = 3$, $t = 6$ mm (total average RSSI = 2878) and Dipole: $\varepsilon_r = 3$, $t = 6$ mm (total average RSSI = 2880). This demonstrates that these designs were the most robust tags observed throughout the measurements which are in line with the results of the simulations. At the other end of the scale, the Dipole: $\varepsilon_r = 3$, $t = 6$ mm M showed unexpectedly very low RSSI values (total average RSSI = 215) throughout the measurements which may have been an error in the etching of the tag or with the soldering of the chip to the antenna, resulting in a mismatch and an increase in transmission losses.

4 Conclusions, limitations, further work and practical implications

The research presented in this paper demonstrates the read range of RFID tags may be accurately predicted from simulation results to enable "Cyber" comparisons of designed tags. The measurements were performed on different materials in MP and NMP scenarios to investigate the robustness of tag performance. The simulation results indicated that tags designed to work for NMP are more robust to changes in permittivity than tags that have been designed for the use of MP components. The measurement results further demonstrated that tags designed to work with NMP are more robust than tags designed with MP when attached directly to the metal surface. Furthermore, the results suggest the Slot design has the potential to work in unknown geometries but requires careful design. The paper contributes to the wider research discussion surrounding the use of simulation efficacy prior to the deployment of IIoT and Industry 5.0 technologies.

Recent research highlights the need for accurate detection of tags when multiple tags are present or to detect those which are absent (e.g. [36, 37]). The tags were assessed for performance as a lone tag; further assessment is needed to determine if the results are replicated with multiple tags. For practical purposes, the physical testing was conducted in a laboratory environment which is not representative of environments in logistics, warehouses or factories. Future work will include testing within industrial environments across different domains. In addition, the focus was on evaluating the efficacy of passive RFID tags; further work is necessary to assess whether the simulation of active and semi-active tags correlates with real-world performance on and not MP. Further work could also explore the effect of handling of the tags on performance in real industrial settings and the location and orientation of the tag on the product.

The practical implications relate to the selection of the most appropriate tag for industrial use. If the same tag is required to work on a variety of products, it is best to use a tag designed not to work MP. However, if tagging of metal products is essential for robust performance, tags would require a dielectric substrate to separate their antennas from the detuning effects of the metal. The results indicated that tags have much higher efficiencies on permittivities that they are designed for, especially in MP scenarios. Therefore, to achieve the highest total efficiency, RFID tags should be designed specifically for the material properties of the products that they are going to be applied to. Although this could result in higher initial production costs and delays, whilst appropriate designs are evaluated, the benefits include more robust, reliable and larger read ranges. The result of these improved tags may include increased confidence in any knowledge derived from analysing the performance of the intelligent products, packaging and processes.

Author contribution Material preparation, data collection and analysis were performed by JT. The first draft of the manuscript was written by JT, and all authors commented on previous versions of the manuscript. All authors read and approved the final manuscript and conducted several edits. SH acted on the reviewer comments and amended the manuscript prior to resubmission, checked by KvL.

Funding This work was supported by EPSRC (Grant number EP/PO27482/1-Future connected smart manufacturing platform). The authors have no other relevant financial or non-financial interests to disclose.

Availability of data and material Data may be made available upon request of the authors.

Code availability N/A.

Declarations

Ethics approval N/A.

Consent to participate N/A.

Consent for publication The authors give consent for this paper to be published.

Conflict of interest The authors declare no competing interests.

References

1. Fraga-Lamas P, Varela-Barbeito J, Fernandez-Carames TM (2021) Next generation auto-identification and traceability technologies for industry 5.0: a methodology and practical use case for the shipbuilding industry. IEEE Access 9:140700–140730. https://doi.org/10.1109/ACCESS.2021.3119775
2. Kagermann H, Wahlster W, Helbig J (2013) Recommendations for implementing the strategic initiative INDUSTRIE 4.0 - Final report of the Industrie 4.0 Working Group
3. Bindel A, Rosamond E, Conway P, West A (2012) Product life cycle information management in the electronics supply chain. Proc Inst Mech Eng Part B: J Eng Manuf 226(8):1388–1400. https://doi.org/10.1177/0954405412448780
4. Lam CY, Ip WH (2019) An integrated logistics routing and scheduling network model with RFID-GPS data for supply chain management. Wireless Pers Commun 105(3):803–817. https://doi.org/10.1007/s11277-019-06122-6
5. Shirehjini AAN, Shirmohammadi S (2020) Improving accuracy and robustness in HF-RFID based indoor positioning with Kalman filtering and Tukey smoothing. IEEE Trans Instrum Meas. https://doi.org/10.1109/TIM.2020.2995281
6. Hayward SJ, Earps J, Sharpe R, van Lopik K, Tribe J, West AA (2021) A novel inertial positioning update method, using passive RFID tags, for indoor asset localisation. CIRP J Manuf Sci Technol 35:968–982. https://doi.org/10.1016/J.CIRPJ.2021.10.006
7. Neal AD et al (2021) The potential of industry 4.0 Cyber Physical System to improve quality assurance: an automotive case study for wash monitoring of returnable transit items. CIRP J Manuf Sci Technol 32:461–475. https://doi.org/10.1016/j.cirpj.2020.07.002
8. Lu S, Xu C, Zhong RY (2016) An active RFID tag-enabled locating approach with multipath effect elimination in AGV. IEEE Trans Autom Sci Eng 13(3):1333–1342. https://doi.org/10.1109/TASE.2016.2573595
9. Welbourne E, Battle L, Cole G (2009) Building the internet of things using RFID: the RFID ecosystem experience. Internet Computing 13(3):48–55
10. Hasan MS, Yu H (2011) Design and simulation of UHF RFID tag antennas and performance evaluation in presence of a metallic surface. 2011 5th International Conference on Software, Knowledge Information, Industrial Management and Applications (SKIMA) Proceedings pp 1–5. https://doi.org/10.1109/SKIMA.2011.6089974
11. Roy AA, Môm JM, Kureve DT (2013) Effect of dielectric constant on the design of rectangular microstrip antenna. 2013 IEEE Int Conf Emerg Sust Technol Power ICT Develop Soc (NIGERCON) pp 111–115. https://doi.org/10.1109/NIGERCON.2013.6715645
12. Bibi F, Guillaume C, Gontard N, Sorli B (2017) A review: RFID technology having sensing aptitudes for food industry and their contribution to tracking and monitoring of food products. Trends Food Sci Technol 62:91–103. https://doi.org/10.1016/j.tifs.2017.01.013
13. Lu BH, Bateman RJ, Cheng K (2006) RFID enabled manufacturing: fundamentals, methodology and applications. Int J Agile Syst Manag 1(1):73–92. https://doi.org/10.1504/IJASM.2006.008860
14. T. Editors of Encyclopeadia Britannica (2016) Dielectric constant. Encyclopaedia Britannica
15. Rialet D, Sharaiha A, Tarot A, Castel X, Delaveaud C (2009) Characterization of antennas on dielectric and magnetic substrates effective medium approximation. Radioengineering 18(4):348–353
16. Lee KF, Luk KM (2011) Microstrip patch antennas. Imperial College Press, 2011
17. Marrocco G (2007) RFID Antennas for the UHF remote monitoring of human subjects. IEEE Trans Antennas Propag 55(6):1862–1870. https://doi.org/10.1109/TAP.2007.898626
18. Pozar DM (1992) Microstrip antennas. Proc IEEE 80(1):79–91. https://doi.org/10.1109/5.119568
19. I GmbH EMPIRE XPU 7
20. Alien Technology (2017) Higgs ™ -3 SOT ALC-360-SOT Datasheet
21. Alien Technology (2014) ALN-9640 Squiggle Inlay. https://www.rfidglobal.it/download/sales/datasheet_apparati_rfid/Transponder-RFID-Passivi/etichette_rfid_uhf_alien/ALN-9640_Squiggle_Higgs3_RFID_Global.pdf. Accessed 19 May 2020
22. Mohammed NA, Demarest KR, Deavours DD (2010) Analysis and synthesis of UHF RFID antennas using the embedded T-match. IEEE Int Conf RFID 2010:230–236. https://doi.org/10.1109/RFID.2010.5467276
23. Ziai M, Batchelor J (2011) Temporary on-skin passive UHF RFID transfer tag. IEEE Trans Antennas Propag 59(10):3565–3571
24. I Corporation (2017) PCB stackup design considerations for Intel FPGAs. pp 1–29
25. Alien Technology (2014) Alr-8696-C

26. Laird. Eccostock ® SH Rigid High Temperature Plastic Foam Sheet Stock
27. R Corporation (2015) RO3000 ® Series Circuit Materials Data Sheet
28. S. silicones Ltd, Solid silicone sheet - GP (2018)
29. Teledynestorm. High performance microwave interconnect products: dielectric options. p 1
30. Omega. RF/capacitance level instrumentation.
31. Elert G. Dielectrics. The Physics Hypertextbook
32. Chen S, Lin K, Mittra R (2010) A measurement technique for verifying the match condition of assembled RFID tags. IEEE Trans Instrum Meas 59(8):2123–2133
33. Svečko J, Malajner M, Gleich D (2015) Distance estimation using RSSI and particle filter. ISA Trans 55:275–285. https://doi.org/10.1016/j.isatra.2014.10.003
34. Malajner M, Cucej Z, Gleich D (2012) Angle of arrival estimation using a single omnidirectional rotatable antenna. 2012 IEEE Int Conf Wireless Information Technol Syst. ICWITS 12(6):1950–1957. https://doi.org/10.1109/ICWITS.2012.6417683
35. Malajner M, Benkic K, Planinsic P, Cucej Z (2009) The accuracy of propagation models for distance measurement between WSN nodes. 2009 16th Int Conf Syst Signals Image Process. IWSSIP pp 9–12. https://doi.org/10.1109/IWSSIP.2009.5367782
36. Yu J, Gong W, Liu J, Chen L, Wang K (2019) On Efficient tree-based tag search in large-scale RFID systems. IEEE/ACM Trans Networking 27(1):42–55. https://doi.org/10.1109/TNET.2018.2879979
37. Yu J, Gong W, Liu J, Chen L, Wang K, Zhang R (2020) Missing tag identification in COTS RFID systems: bridging the gap between theory and practice. IEEE Trans Mob Comput 19(1):130–141. https://doi.org/10.1109/TMC.2018.2889068